Published article:
Harput, S, Evans, T, Bubb, N and Freear, S (2011) *Detection of Restoration Faults under Fillings in Human Teeth using Ultrasound.* In: IEEE International Ultrasonics Symposium. 2011 IEEE International Ultrasonics Symposium (IUS), 18-21 October 2011, Orlando, Florida, USA. IEEE.

http://dx.doi.org/10.1109/ULTSYM.2011.0357

Detection of Restoration Faults under Fillings in Human Tooth using Ultrasound

Sevan Harput, Tony Evans[†], Nigel Bubb[‡], and Steven Freear

Ultrasound Group, School of Electronic and Electrical Engineering, University of Leeds, UK.
[†]Division of Medical Physics, University of Leeds, UK. [‡]Oral Biology, University of Leeds, UK.
E-mail: S.Harput@leeds.ac.uk and S.Freear@leeds.ac.uk

***Abstract*—An ultrasound contact imaging technique for detecting the restoration faults under the fillings in human tooth is proposed. A linear frequency modulated chirp signal is used to improve the signal-to-noise ratio and increase the penetration depth to allow the detection of the echoes from restoration-tooth boundary at 200 kPa acoustic pressure. Although the detection threshold is improved, it is observed that the duration of the excitation signal is longer than the duration of time of flight in the restoration, which causes signal overlapping between consecutive internal reflections. Due to these reverberations, the applied chirp signals interfere arbitrarily with the successive reflections, where the received echoes are not identifiable in the time domain. Separation in the frequency domain is not possible, since all reflections have the same bandwidth and the center frequency.**

In this work, the fractional Fourier transform (FrFT) is employed to separate chirp signals overlapping in both time and frequency domains. By analyzing the received echoes with FrFT, this work presents the ultrasonic non-destructive evaluation of dental restorations in human teeth.

I. Introduction

One of the major problems encountered in tooth restoration is the bonding faults between the restoration material and tooth. The restorative insertion placed in the tooth must completely reach the base and form a flawless bond, otherwise a cavity will be created inside the tooth, which can cause an infection requiring repetition of the restoration procedure [1]. Small cavities are challenging for conventional X-ray imaging, because dental radiographs are usually not effective in the early detection but often rely on the subsequent damage after infection [2]. However ultrasound is highly effective in detecting discontinuities in the tooth, even if they are smaller than the acoustic wavelength. The advantage of the ultrasound becomes more apparent if the restoration material is radiopaque and hence cannot be imaged by conventional radiography. Ultrasound however is able to penetrate the hard structures and can detect hard tissue pathosis and cavities under existing restorations [3], [4].

The aim of this work is to detect the possible restoration faults under fillings in human tooth using ultrasound. Linear frequency modulated (LFM) chirp signal is chosen for excitation to increase the penetration depth. On the receiver side, the fractional Fourier transform (FrFT) is used to filter the received echoes and separate overlapping LFM chirps.

II. Methodology

A. Coded Excitation

It has already presented by Singh *et al.* that ultrasound can penetrate most of the dental restorative materials such as amalgam, resin-composite, porcelain and gold [4]. However, the authors observed that gold restorations transmit minimal acoustic energy to the tooth behind the restoration due to their large acoustic impedance. In this study, a coded excitation technique is chosen to overcome such penetration problems.

Coded excitation has been effectively used in radar applications and medical ultrasound systems to improve the image quality [5]. However, the usage of coded excitation in echodentography is not common except some recent studies [6], [7]. In this work, an LFM chirp is used as an excitation signal to improve the signal-to-noise ratio (SNR) and penetration depth.

B. Power of Received Echo

The power level of the received echo can be estimated by using the acoustic impedance and attenuation coefficient of the medium in which the ultrasonic wave is travelling with the material properties given in Table I. The transmitted ultrasonic wave into the restoration, which has exactly 3 dB less energy than the incident wave for this case, reflects from the back of the restoration-dentin boundary with different power levels according to the quality of the bonding.

The received signal power is reduced as determined by the reflection coefficient, Γ, and the reflected echoes are further attenuated by 1 dB/mm in the resin based restorative material. Therefore, the total power of the echo can be calculated as

$$\text{Received Power}_{(\text{dB})} = -10\log(\Gamma^2) - \text{Attenuation}_{(\text{dB})} \quad (1)$$

for

$$\Gamma = \frac{\mathrm{Z}_1 - \mathrm{Z}_0}{\mathrm{Z}_1 + \mathrm{Z}_0} \quad (2)$$

where the wave is propagated from medium of impedance Z_0 into a medium of impedance Z_1.

The main problem with this type of techniques based on reflected power calculations is that the received signal must be compressed accurately. However for the tooth measurements, the received signal's energy is still spread in time after compression with a matched filter (MF). The compression is

TABLE I
ACOUSTIC PROPERTIES OF MATERIALS

MATERIAL	Velocity (m/s)	Attenuation (dB/mm)	Impedance (MRayl)
Dentin	3800[d]	8[c]	7.6[d]
Restorative Material	3530[a]	1[a]	14.5[a]
Glycerin	1910[a]	-	2.42[a]
Delay-line, polystyrene	2310[a]	0.18[b]	2.47[a]

[a] values are determined in our laboratory. [b] values are taken from [9].
[c] values are measured by Kossoff and Sharpe at 18 MHz [10].
[d] values are compiled by Ghorayeb *et al.* [11].

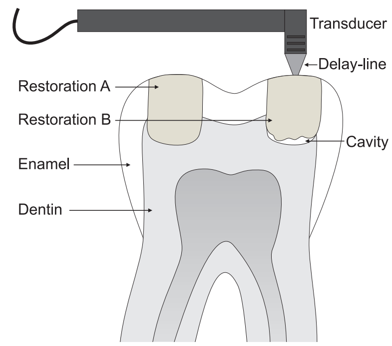

Fig. 1. Experimental Setup.

not ideal, since the received signal is deformed because of frequency dependant attenuation, scattering and dispersion in tooth layers and dental restorative material [8]. The overall effect on the received echo is usually observed as change in the envelope shape and reduction in the bandwidth, which will result in a discrepancy between the MF and chirp signal. For this reason, rather than measuring the peak power of the compressed signals, the total power of individual echoes is calculated in time domain after separating with the FrFT as

$$\text{Power} = \frac{1}{t_2 - t_1} \int_{t_1}^{t_2} x(t)^2 dt \, . \tag{3}$$

C. Fractional Fourier Transform (FrFT)

The coded excitation improves the penetration and SNR, but introduces another problem when the duration of the ultrasound signal is longer than the time of the round trip in the restorative material. Due to the signal overlapping inside the restorative material, the received echoes are not identifiable in the time domain. In the frequency domain all reflections completely overlap with each other, since they all have the same bandwidth and the center frequency. The proposed solution in this work is to use the fractional Fourier transform with long duration LFM chirp excitation. The FrFT allows frequency modulated signals overlapping in time and frequency to be separated.

The Fourier transform can be re-written in the generalized form as follows

$$X_\alpha \left(t_\alpha\right) = \int_{-\infty}^{\infty} x(t) \, B_\alpha(t_\alpha, t) \, dt \tag{4}$$

where the it is the same with traditional Fourier transform for

$$B(f, t) = \exp(-j2\pi f t) \, . \tag{5}$$

When the transform kernel is modified as [12]

$$B_\alpha(t_\alpha, t) = B_\phi \exp\left[j\pi \left(t_\alpha^2 \cot\phi - 2 t_\alpha t \csc\phi + t^2 \cot\phi\right)\right] \tag{6}$$

where

$$B_\phi = |\sin\phi|^{-1/2} \exp\left[\frac{-j\pi \, \mathrm{sgn}(\sin\phi)}{4} + j\frac{\phi}{2}\right] \tag{7}$$

and $\phi = \alpha\pi/2$, the transformation becomes the fractional Fourier transform. The α defines the order of the transform, $B_\alpha(t_\alpha, t)$ is the transform kernel and t_α denotes the variable in the α-th order fractional Fourier domain. The FrFT enables transformation on to any line of angle in time-frequency space.

For an LFM signal the chirp rate, a, equals to B/T, where B is the bandwidth and T is signal duration. When analyzing overlapped LFM signals, the FrFT can be used to separate the signals by rotating the waveform to another domain between time and frequency. The transform order is optimum when it is matched to the chirp rate of the signal where maximum compression is achieved in the fractional projection. The waveform can be rotated in the fractional domain by the optimum transform order α_{opt}, which is defined as [13]

$$\alpha_{opt} = -\frac{2}{\pi} \tan^{-1}\left(\frac{\Delta f / \Delta t}{2a}\right) \, , \tag{8}$$

where Δf and Δt are the frequency and time resolutions.

In this work, to isolate individual chirp signals windowing is used in the fractional domain. Recently presented by Cowell *et al.*, after windowing in fractional domain the waveform can be rotated by $-\alpha_{opt}$ degrees to restore the signal to the time domain hence extracting the chirp from overlapped data [14].

III. EXPERIMENTS

A. Experimental Setup

A dentist performed two different restorations on an extracted human molar. Two cylindrical cavities were formed using a dental drill on the tooth crown with a depth of 2.4 mm. Dental composite Herculite XRV Unidose enamel (Kerr) was used as the restoration material. For restoration **A**, a bonding agent was applied before filling the cavity with restorative material. However, for restoration **B**, in order to create a poor filling, the cavity was covered with glycerin. After filling the cavities, restorative material was cured by UV light and the surfaces of the fillings were flattened using dental instruments. After the restoration process, the tooth sample was scanned by the X-ray scanner μCT 80 (Scanco Medical AG) with 40 μm resolution. Fig. 2 shows the X-ray scan of the tooth with restorations. The shape of the filling on the left hand side of the X-ray image matches this cavity shape. However, for the filling on the right hand side it can be observed on the bottom of the cavity that it is not bonded well with the dentin.

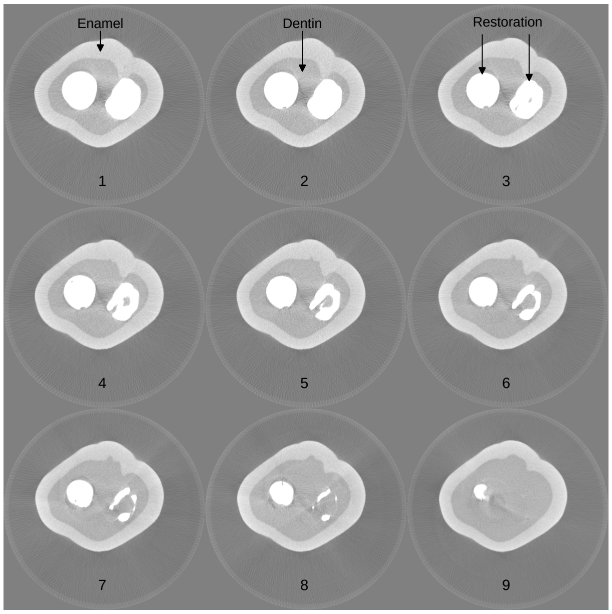

Fig. 2. X-ray image of tooth with restorations. Each scan is separated by 80 μm and the scan direction is from crown to the root of the tooth.

The measurements were carried out by a 15 MHz Sonopen Delay Line Transducer with 1 mm polystyrene tip (Olympus NDT Inc.) using a glycerin couplant in contact mode as shown in Fig. 1. The excitation signal was designed to match the transducer frequency response, and therefore a center frequency of 14 MHz and a fractional bandwidth of 80% are chosen. The excitation voltage of 25 V was used with a signal duration of 2 μs, which generates a pressure of 200 kPa. The excitation signal was tapered with a Hann window to reduce the side lobe levels after compression. A 33250A Arbitrary Waveform Generator (Agilent Tech. Inc.) was programmed to generate the excitation signal and then amplified by using E&I A150 RF Power Amplifier (E&I Ltd.). The received signal was amplified by 50 dB with a Panametrics 5072PR (Olympus NTD Inc.) after separating the transmitted and received signals by a RDX-6 diplexer (Ritec Inc.). The received ultrasound echoes from the tooth sample were saved by a Waverunner 64xi Oscilloscope (LeCroy Corp.) and signals were processed in Matlab (Mathworks Inc.). The contact mode imaging and the importance of glycerin couplant is explained in [7].

In order to perform the ultrasound scan, the tooth sample was fixed on a stationary stage and transducer is held by a mounting frame on the high precision CNC positioning system. The tooth sample was scanned by the automated CNC with a step size of 0.5 mm through the surface of both fillings on the scan lines **A** and **B** as shown in Fig. 5.

B. Filtering with FrFT

To separate the interfered chirp signals, the LFM measurements were processed using the FrFT or MF technique. The matched filter was chosen, since it is the most common method for filtering and compressing chirp signals, where it optimizes the probability of the detection and maximizes the SNR [5].

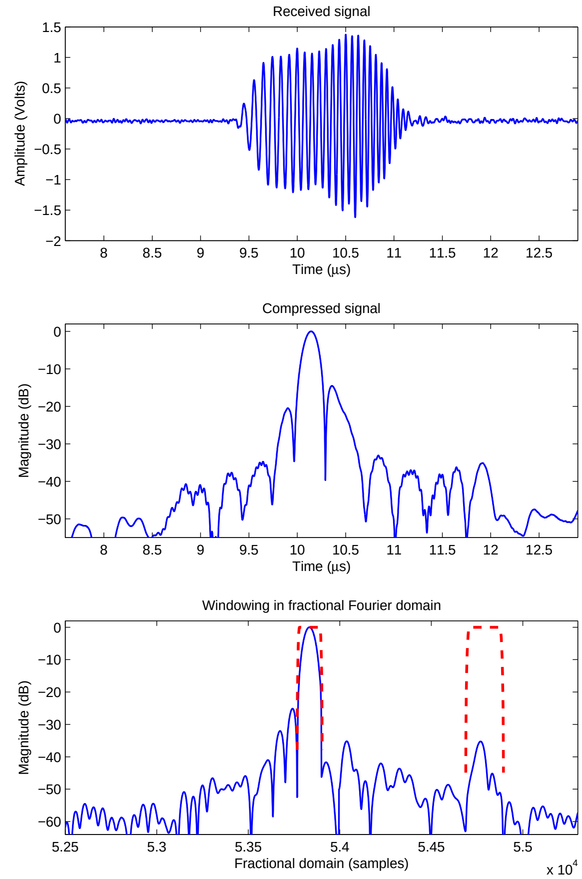

Fig. 3. (Top) Received signal. (Middle) Compression with MF. (Bottom) Transformation into fractional Fourier domain.

The received signal, shown in Fig. 3 (top), was first processed with MF. However, it was not possible to distinguish the reflection from restoration-dentin boundary clearly from the compressed signal shown in Fig. 3 (middle).

The FrFT was performed at $\alpha = 1.336$, where the rotation angle was calculated according to Eq. (8). Unlike the MF, the first echo from the transducer-restoration boundary and the second echo from the restoration-dentin boundary were clearly visible in the fractional Fourier domain. The individual echoes were separated by windowing as shown in Fig. 3 (bottom), and the filtered signal was transformed back to the time domain by applying the inverse FrFT [14]. The separated chirps are plotted in Fig. 4, where the total power of the signals were calculated by integrating in time domain using Eq. (3).

C. Experimental Results

The reflected echoes from the bottom of the fillings are normalized and the power level of the reflected echoes are plotted in Fig. 6 for each scan lines.

$$-10\log\left(\frac{7.6-14.5}{7.6+14.5}\right)^2 - (1\ \text{dB/mm}\times 4.8\ \text{mm}) = -14.91\ \text{dB}.$$

By assuming a perfect reflector geometry, a threshold value of -14.91 dB is calculated for a good bonding according to Eq. (1) by using the material properties given in Table I.

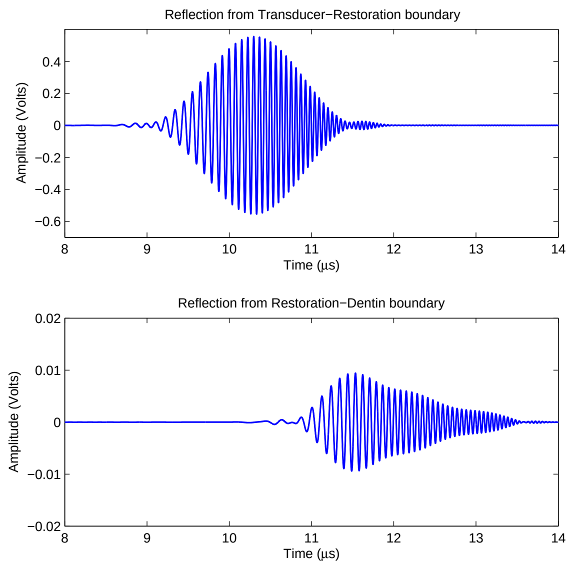

Fig. 4. Received signal after filtering in fractional Fourier domain.

The maximum power of reflected echo observed for the scan line **A** was -17.3 dB, which is below the threshold and does not indicate any bonding problems. For the scan line **B**, the echoes between 3.0 mm and 4.5 mm show the reflections from the bottom of the filling and the reflected power was between -13.1 dB and -7.8 dB. For restoration **B**, the reflections from the filling was always above the threshold for each scan point, which shows an adhesion problem between filling and tooth.

IV. Conclusions

Radiography is currently used as a diagnostic technique in dentistry, but it is not ideal for dental imaging due to its ionizing nature. However ultrasound, a non-ionizing modality, can be safely used for dental measurements to locate discontinuities inside the tooth at low pressure levels. In this study, the ultrasonic non-destructive evaluation of restorations in human teeth using chirp coded excitation was performed. The FrFT was used to analyze the received echoes by separating chirp signals overlapping in both time and frequency domains.

V. Acknowledgment

The use of human teeth was approved by the Leeds Dental Institute Skeletal Tissues Bank (ref: 07H130693). Authors would like to thank Prof. R. M. Hall, Khalid Sindi, and Ondrej Holub of University of Leeds for their help in this study.

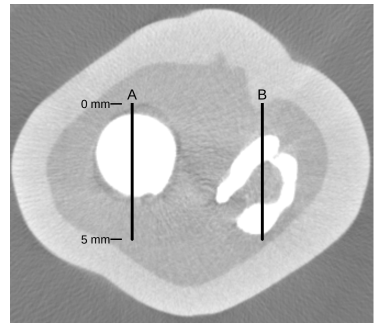

Fig. 5. Scan lines for the ultrasound measurements.

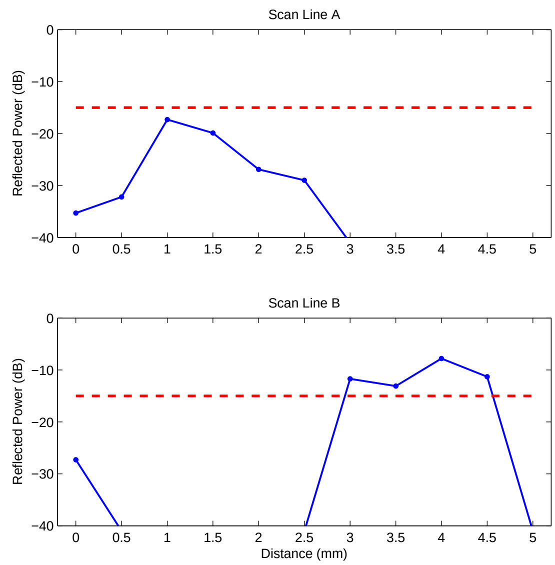

Fig. 6. The power of echoes from the bottom of the fillings for scan lines **A** and **B**. Red dashed line shows the detection threshold for restoration failures. Signal power above this threshold indicates a bonding problem.

References

[1] S. Ghorayeb and T. Valle, “Experimental evaluation of human teeth using noninvasive ultrasound: echodentography,” *IEEE Trans. UFFC*, vol. 49, no. 10, pp. 1437–1443, 2002.

[2] M. O. Culjat *et al.*, “Ultrasound crack detection in a simulated human tooth,” *Dentomaxillofac Radiology*, vol. 34, no. 2, pp. 80–85, 2005.

[3] M. Culjat, R. Singh, D. Yoon, and E. Brown, “Imaging of human tooth enamel using ultrasound,” *Medical Imaging, IEEE Transactions on*, vol. 22, no. 4, pp. 526–529, 2003.

[4] R. Singh *et al.*, “Penetration of radiopaque dental restorative materials using a novel ultrasound imaging system,” *American Journal of Dentistry*, vol. 20, no. 4, pp. 221–226, 2007.

[5] T. Misaridis and J. Jensen, “Use of modulated excitation signals in medical ultrasound. part i: basic concepts and expected benefits,” *IEEE Trans. UFFC*, vol. 52, no. 2, pp. 177–191, 2005.

[6] S. Harput, D. M. J. Cowell, J. A. Evans, N. Bubb, and S. Freear, “Tooth characterization using ultrasound with fractional Fourier transform,” in *IEEE Ultrasonics Symposium*, 2009, pp. 1906–1909.

[7] S. Harput, T. Evans, N. Bubb, and S. Freear, “Diagnostic ultrasound tooth imaging using fractional Fourier transform,” *IEEE Trans. UFFC*, vol. 58, no. 10, pp. 2096–2106, 2011.

[8] F. Barber, S. Lees, and R. Lobene, “Ultrasonic pulse-echo measurements in teeth,” *Archives of Oral Biology*, vol. 14, no. 7, pp. 745–760, 1969.

[9] G. S. Kino, *Acoustic Waves:Devices, Imaging, and Analog Signal Processing*, R. Woods, Ed. Prentice-Hall, Inc., 1987.

[10] G. Kossoff and C. Sharpe, “Examination of the contents of the pulp cavity in teeth,” *Ultrasonics*, vol. 4, no. 2, pp. 77–83, 1966.

[11] S. Ghorayeb, C. Bertoncini, and M. Hinders, “Ultrasonography in dentistry,” *IEEE Trans. UFFC*, vol. 55, no. 6, pp. 1256–1266, 2008.

[12] H. Ozaktas, O. Arıkan, M. Kutay, and G. Bozdağı, “Digital computation of the fractional Fourier transform,” *IEEE Trans. Signal Processing*, vol. 44, no. 9, pp. 2141–2150, 1996.

[13] C. Capus and K. Brown, “Short-time fractional Fourier methods for the time-frequency representation of chirp signals,” *Journal of the Acoustical Society of America*, vol. 113, no. 6, pp. 3253–3263, 2003.

[14] D. Cowell and S. Freear, “Separation of overlapping linear frequency modulated (LFM) signals using the fractional Fourier transform,” *IEEE Trans. UFFC*, vol. 57, no. 10, pp. 2324–2333, 2010.